

ROLE OF MAGNETIC FIELD AND DENSITY GRADIENTS IN RAYLEIGH-TAYLOR INSTABILITY OF LASER PRODUCED PLASMAS

*M. K. AYUB and S. MAHMOOD

Theoretical Plasma Physics Division, PINSTECH, P.O.Nilore, Islamabad, Pakistan

(Received July 27, 2009 and accepted in revised form November 25, 2009)

Hydrodynamic equations of laser produced plasmas are presented and solved to calculate the linear growth rate of Rayleigh-Taylor instability (RTI) by using normal mode analysis. The growth rates of RTI are calculated in the absence and presence of the external magnetic field. The growth rates are presented graphically against the perturbation wavelength for different angles between the wave vector and initial horizontally directed magnetic field. The dependence of RTI growth rate on the interface density gradient and ablation effects is also investigated. It is found that growth rate of RTI is decreased in the presence of magnetic field; interface density gradient and ablation effects in laser produced plasmas. The numerical results are also presented and found to be in good agreement with the experimental observations.

Keywords: Rayleigh-Taylor instability, Magnetic effects on RTI, Ablation surface instability, Density gradient effects in RTI, ICF problems.

1. Introduction

The Rayleigh-Taylor instability (RTI) in plasmas is produced, when a heavy fluid supported by a light fluid is in equilibrium in a gravitational field [1]. During this equilibrium, if a small perturbation is introduced then this perturbation will grow and causing the system towards RTI. The instability occurs because any exchange of position between two elements with equal volume of the two fluids leads to a decrease of the potential energy of the system [2]. In general one gets RT stability when a light fluid pushes and accelerates a heavy fluid as shown in Fig. 1. In laser plasmas interaction, the RTI occurs whenever a pressure gradient opposes a density gradient i.e. $\vec{\nabla}P$ is in an opposite direction to $\vec{\nabla}\rho$ [3].

Let us consider two superimposed fluids, with densities ' ρ_H ' (heavy fluid) and ' ρ_L ' (light fluid); separated by a horizontal boundary and subjected to gravity 'g'. The fluids are in hydrostatic equilibrium. However, when the upper fluid is heavier than the lower one, the small perturbations at the interface rapidly grow in time. Soon spikes of the heavier fluid fall down, while bubbles of the lighter fluid rise as shown in Fig. 2.

A sinusoidal wave, with amplitude ' ξ ' on the surface between the two RT unstable fluids will grow exponentially, which is given by

$$\xi = \xi_0 \exp(\gamma t) \quad (1)$$

Where

$$\gamma = \sqrt{Aka}, \quad A = \left(\frac{\rho_H - \rho_L}{\rho_H + \rho_L} \right) \text{ and } k = \frac{2\pi}{\lambda} \text{ have}$$

been defined as growth rate, Atwood number and wave vector respectively, and 'a' is the acceleration of the two fluids (or $a=g$ in the gravitational field, without acceleration).

For ICF, the low-density, high-pressure ablating plasma accelerates the high-density shell and $\rho_H \gg \rho_L$ so the Atwood number is close to one. The growth rate defined in Eq. (1) does not take into account the density gradient effects. However, if we consider the density gradient at the interface of heavy and lighter fluid, it can have a stabilizing effect and explained with an effective Atwood number. The growth rate of RTI with density gradient at the interface is given by

*Corresponding author : kpieas84@yahoo.com

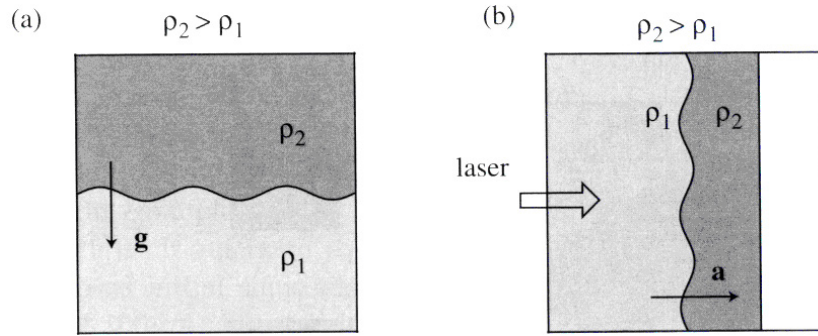


Figure 1. Rayleigh Taylor unstable interface between the fluids of different densities: a) a lighter fluid supports a heavier fluid in gravitational field; 2) a lighter fluid pushes and accelerates a layer of denser fluid in laser produced plasma [4].

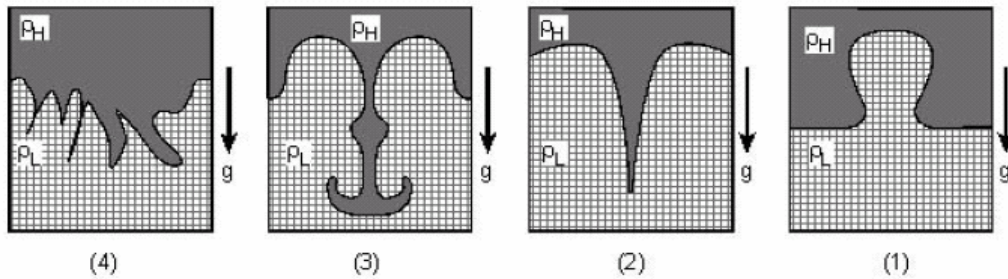


Figure 2. Characteristic flow patterns in the evolution of RT instability: 1) a bubble formation penetrating the heavy fluid, 2) a spike entering in low density medium, 3) a spike formation with vortex motion, 4) intermixing between the fluids [3].

$$\gamma = \sqrt{\frac{gk}{1+kL}} \quad (2)$$

Where $L = \frac{\rho}{\nabla\rho}$ is called the scale length of density gradient at the interface [7]. Here it is worthy to note that the growth rate described in Eq. (2) decreases with the increasing in the value of L .

In inertial confinement fusion (ICF), interaction of an intense laser with solid matter causes ablation of the solid and generation of ablative pressure. Ablative pressure can be used to accelerate thin targets. The most important application of ablative pressure is driving the implosion of spherical shell targets for the achievement of inertial confinement fusion reactions [5]. However, the ablation front, which separates the low density hot plasma from the accelerated dense layer, is hydrodynamically unstable. Under these conditions RTI can occur thus hindering the compression of the solid matter

[6]. The determination of the RTI growth rate is crucial for the success of ICF because an excessive distortion of the ablation front could lead to a severe degradation of the capsule performance with respect to the final core conditions by seeding RTI during the deceleration phase and prevent the onset of the ignition process [10].

In 1973 an early paper out of the Naval Research Laboratory (NRL) reported that accurate dispersion relation including ablation and density gradient effects at the interface still did not exist to describe the RTI growth rate. Furthermore, the nonlinear growth and turbulence properties were almost entirely a mystery. A theoretical understanding of ablative stabilization was gradually evolved and confirmed by experiments. The linear growth of RTI was well understood with good agreement between experiment and simulation for planar geometry with wavelengths in the region of 30-100 μm [7].

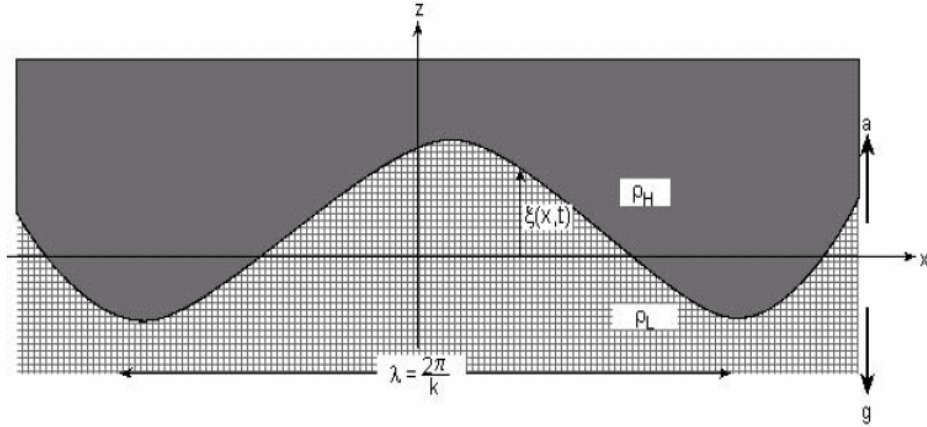


Figure 3. Rayleigh-Taylor instability in the presence of gravitation g (down) or acceleration a (up) [3].

Recently, the growth of RTI with plastic target of solid density has been studied intensively. The wave number dependence of the growth rate has been well studied but the target density dependence of the RT growth rate has not been investigated. This study is important for various mitigation schemes of the RT instability, such as stability using picket pulses, high-Z coating, double ablation and cocktail color irradiation [11]. It has also been observed that RTI plays an important role in many complex phenomenons, such as some stages of stellar evolution, fragmentation of vapor films, deceleration of laser generated plumes, underground salt domes and volcanic islands etc. [3].

The layout of the paper is presented as follow: In Sec.II different models and set of equations are presented to study RTI in laser produced plasmas. The analytical expressions of their growth rates are also obtained in the linear limit. In Sec.III, the numerical plots are drawn for ICF experiments. A conclusion is presented in Sec.IV.

2. Models and Set of Equations

2.1. Rayleigh-Taylor Instability in unmagnetized plasmas : A linear analysis

In order to study the linear analysis of RTI [3], we consider the hydrodynamic equations describing the fluid motion. The mass conservation equation is described as

$$\frac{\partial \rho}{\partial t} + \nabla \cdot (\rho \vec{v}) = 0 \quad (3)$$

and momentum conservation equation is given by

$$\rho \frac{\partial \vec{v}}{\partial t} + \rho (\vec{v} \cdot \nabla) \vec{v} = -\nabla P + \rho \vec{g} \quad (4)$$

Where ρ is the fluid density, \vec{v} is the flow velocity, P is the pressure and $\rho \vec{g}$ is the external force acting on the fluid (if there is an acceleration, then $\vec{a} = -\vec{g}$). The Cartesian coordinates with unit vectors \hat{x} , \hat{y} and \hat{z} are used, and the gravitational field (or the acceleration) is perpendicular to the interface between the fluids as shown in Fig. 3.

Therefore

$$\vec{g} = -g \hat{z}$$

In the linear approximation, we have

$$\begin{aligned} \rho &= \rho_0 + \rho_1 & \rho_0 &\gg \rho_1 \\ \vec{v} &= \vec{v}_0 + \vec{v}_1 & \vec{v}_0 &\gg \vec{v}_1 \\ P &= P_0 + P_1 & P_0 &\gg P_1 \end{aligned} \quad (5)$$

Substituting Eq. (5) in Eq. (3) and Eq. (4), with stationary fluid assumptions, and on solving, we get the following two equations after linearization, described as follows,

$$\frac{\partial \rho_1}{\partial t} + \nabla \cdot (\rho_0 \vec{v}_1) = 0 \quad (6)$$

$$\rho_0 \frac{\partial \vec{v}_1}{\partial t} + \vec{\nabla} P_1 - \rho_1 \vec{g} = 0 \quad (7)$$

We take incompressible flow assumption, i.e. density of the fluid is constant with time. The incompressible flow assumption is a reasonable approximation for fluids having flow velocities much less than the local speed of sound. Therefore, in Lagrangian coordinate system we can write

$$\frac{d\rho}{dt} = \frac{\partial \rho}{\partial t} + \vec{v} \cdot \vec{\nabla} \rho = 0 \quad (8)$$

Using linearization approximation in Eq. (8), together with Eq. (6) we obtain the following two equations as follows

$$\frac{\partial \rho_1}{\partial t} + \vec{v}_1 \cdot \vec{\nabla} \rho_0 = 0 \quad (9)$$

$$\vec{\nabla} \cdot \vec{v}_1 = 0 \quad (10)$$

On solving Eqs. (9) and (10) together with Eq. (7), with assumption that initial density ρ_0 is constant in both fluids and changes only in the z-direction, i.e. normal to the interface between the fluids i.e. $\frac{\partial \rho_0}{\partial x} = 0, \frac{\partial \rho_0}{\partial y} = 0$ and $\frac{\partial \rho_0}{\partial z} \neq 0$. Writing Eqs. (7), (9) and (10) explicitly in Cartesian coordinates, one gets

$$\begin{aligned} \rho_0 \frac{\partial v_{1x}}{\partial t} + \frac{\partial P_1}{\partial x} &= 0 \\ \rho_0 \frac{\partial v_{1y}}{\partial t} + \frac{\partial P_1}{\partial y} &= 0 \\ \rho_0 \frac{\partial v_{1z}}{\partial t} + \frac{\partial P_1}{\partial z} + \rho_1 g &= 0 \end{aligned} \quad (11)$$

$$\frac{\partial \rho_1}{\partial t} + v_{1z} \frac{\partial \rho_0}{\partial z} = 0$$

$$\frac{\partial v_{1x}}{\partial x} + \frac{\partial v_{1y}}{\partial y} + \frac{\partial v_{1z}}{\partial z} = 0$$

We have five equations with five unknowns $v_{1x}, v_{1y}, v_{1z}, P_1$ and ρ_1 . It is convenient to solve these equations after a Fourier transforms in x-y plane, or equivalently the disturbance is analysed by its normal modes, and solutions depending on x, y and t can be described in the following way.

$$\left. \begin{aligned} v_1(x, y, z, t) &= u(z) \\ P_1(x, y, z, t) &= \delta P(z) \\ \rho_1(x, y, z, t) &= \delta \rho(z) \end{aligned} \right\} \exp i(k_x x + k_y y - \omega t) \quad (12)$$

Where ω is the wave frequency and k_x, k_y are wave numbers along x & y direction such that [3];

$$k^2 = k_x^2 + k_y^2 \text{ where } k = \frac{2\pi}{\lambda}$$

Substituting Eq. (12) into Eq. (11) and after some mathematical manipulations we get following equation in one variable u_z i.e.,

$$\frac{d}{dz} \left(\rho_0 \frac{du_z}{dz} \right) - \left[k^2 \rho_0 + \left(\frac{k^2 g}{\omega^2} \right) \frac{d\rho_0}{dz} \right] u_z = 0 \quad (13)$$

If we assume that the fluid is confined between two rigid planes at $+z_B$ and $-z_B$, then boundary conditions are;

$$\begin{aligned} u_z(\pm z_B) &= 0 \\ \left(\frac{du_z}{dz} \right)_{\pm z_B} &= 0 \end{aligned}$$

The interface is the surface at $z = 0$ and the density is assumed to be constant anywhere except between the fluids at $z = 0$. Therefore, for $z \neq 0$, Eq. (13) can be written as

$$\frac{\partial^2 u_z(z)}{\partial z^2} - k^2 u_z(z) = 0$$

The general solution of this equation can be written as

$$u_z(z) = \alpha \exp(kz) + \beta \exp(-kz)$$

Since u_z vanishes at the boundary and the velocity is continuous at the interface, then one has the solution of the form

$$u_z(z) = \begin{cases} w \exp(+kz) & \text{for } z < 0 \\ w \exp(-kz) & \text{for } z > 0 \end{cases} \quad (14)$$

Now integrating Eq. (13) across the interface from $-\varepsilon$ to $+\varepsilon$, where ε is an infinitesimal element of z . Using solution given in Eq. (14) and denoting the density of the fluid above and below the interface by ρ_{up} and ρ_{down} accordingly (the direction up and down is determined by the direction of g), the Eq. (13) can be written as

$$\int_{-\varepsilon}^{+\varepsilon} \frac{d}{dz} (\rho_0 \frac{\partial u_z}{\partial z}) dz - \int_{-\varepsilon}^{+\varepsilon} k^2 \rho_0 u_z dz - \int_{-\varepsilon}^{+\varepsilon} \frac{gk^2 u_z d\rho_0}{\omega^2 dz} dz = 0$$

In above equation 2nd term disappears because u_z vanishes at the boundary and the velocity is continuous at the interface, otherwise an infinite acceleration is needed to cross the interface. The integration of 1st and 3rd terms is given in Appendix. After solving the above integral equation, we obtained the quadratic equation in ω described as follows,

$$\omega^2 = -Akg$$

Where $A = \frac{(\rho_{up} - \rho_{down})}{(\rho_{up} + \rho_{down})}$ is called the *Atwood number* (a dimensionless parameter). The angular frequency ω is defined as $\omega = \omega_R + i\gamma$, where $\gamma = \sqrt{Akg}$ is a real number describe the growth rate of RTI. Final solution becomes

$$v_z(x, y, z, t) = \begin{cases} w \exp[i(k_x x + k_y y - \omega t)] \exp(+kz) & \text{for } z < 0 \\ w \exp[i(k_x x + k_y y - \omega t)] \exp(-kz) & \text{for } z > 0 \end{cases} \quad (15)$$

Now there are two cases, one is if $\rho_{up} > \rho_{down}$ then A is positive, ω becomes an imaginary number and $\gamma > 0$, then perturbation

grows exponentially and interface becomes unstable [8]. On the other hand, if $\rho_{up} < \rho_{down}$ then A is negative, ω becomes real number and $\gamma < 0$, causing the interface to oscillate and there will be no growth of the perturbation.

2.2. Effects of ablation in RT instability

The effects of ablating material become important when there is an additional flow of material across the ablation surface from the high-density region into the low-density plasma [3]. The following assumptions have been made in the model, i.e. fluid is assumed to be incompressible, the spatial extent and the density gradient of the plasma are neglected, and the plasma heating is not taken into account.

It is assumed that there is a sharp density jump at the interface, so that the density is described by a θ function given as.

$$\rho_0(z) = \rho_{P1} \theta(-z) + \rho_{foil} \theta(z) \quad (16)$$

Where

$$\theta(z) = \begin{cases} 1 & \text{for } z > 0 \\ 0 & \text{for } z < 0 \end{cases}$$

In the foil reference frame of coordinates (the foil is at rest in this frame), the ablated material (plasma) moves with velocity v_{P1} in the $-\hat{z}$ direction (\hat{z} is a unit vector in the z - direction) given as;

$$v_0 = -v_{P1} \theta(-z) \hat{z} = \begin{cases} -v_{P1} \hat{z} & \text{for } z > 0 \\ 0 & \text{for } z < 0 \end{cases} \quad (17)$$

The mass conservation and momentum conservation equations after linear approximation are combined to give as follows.

$$\rho_0 \left(\frac{\partial \vec{v}_1}{\partial t} + \vec{v}_1 \cdot \vec{\nabla} \vec{v}_0 + \vec{v}_0 \cdot \vec{\nabla} \vec{v}_1 \right) = \frac{\rho_1}{\rho_0} \vec{\nabla} P_0 - \vec{\nabla} P_1 \quad (18)$$

Combining Eqs. (8), (9), and (10) along with the incompressibility assumption equations and then

after some mathematical manipulations we get the following equation in one variable u_z as follows,

$$\frac{\partial}{\partial z} \left(\rho_0 \frac{\partial u_z}{\partial z} \right) - \frac{k^2 \rho_0 v_{0z}}{\omega} \frac{\partial u_z}{\partial z} - \left[k^2 \rho_0 + \frac{ak^2}{\omega^2} \frac{\partial \rho_0}{\partial z} + i \frac{k^2 \rho_0}{\omega} \frac{\partial v_{0z}}{\partial z} \right] u_z = 0 \quad (19)$$

Where the acceleration 'a' is defined as, $a = -\left(\frac{1}{\rho_0}\right) \frac{\partial P_0}{\partial z}$. Equation (19) is now integrated

across the interface from $-\varepsilon$ to $+\varepsilon$, where ε is an infinitesimal element of z . The density and initial velocity are described by a θ function, and the derivative of these terms gives the Dirac Delta function defined as $\frac{d\theta(z)}{dz} = \delta(z)$. The integral of the Dirac function over the segment, including the zero of the argument, is equal to one, while the integral of regular functions and the θ function from $-\varepsilon$ to $+\varepsilon$ is equal to zero. In Eq. (19) the integral of 2nd and 3rd term vanish while the integral of 1st, 4th and 5th term is given in Appendix.

After some mathematics, we obtain the following quadratic equation

$$\omega^2 + i\left(\frac{kv_{p1}}{2}\right)\omega + akA = 0$$

The solution of this quadratic equation is

$$\omega = -i\frac{kv_{p1}}{4} \pm \sqrt{\left(i\frac{kv_{p1}}{4}\right)^2 - akA}$$

Here we have assumed

$$-akA \ll \left(\frac{ikv_{p1}}{4}\right)^2 \Rightarrow v_{p1} \ll 4\sqrt{\frac{Aa}{k}}$$

Then above solution becomes

$$\omega \approx \sqrt{-akA} - i\frac{kv_{p1}}{4} + \dots$$

$$\omega = \pm i\left(\sqrt{Aka} - \frac{k}{4}v_{p1}\right)$$

$\gamma = \left(\sqrt{Aka} - \frac{k}{4}v_{p1}\right)$ From this result one can see that the ablation process in laser produced plasmas reduces the growth rate of the Rayleigh-Taylor instability.

2.3. Different models for ablation effects in RT instability

In 1974 Bodner [5] formulated a simple model for the ablation situation with a discontinuity in the density, which shows that the growth rate of the instability is reduced below the classical value by kv_{abl} as given below,

$$\gamma = \sqrt{ka} - kv_{abl} \quad (20)$$

where $v_{abl} = v_{p1}$ is the flow velocity across the ablation front. But relation for continuous density gradient case is different. Gamaly in 1993 [5] derived the following expression,

$$\gamma = \sqrt{\frac{ka}{1+kL}} - kv_{abl} \quad (21)$$

This includes both the ablation velocity and the continuous density gradient in the calculations. However, experimental results and numerical simulations have indicated larger stabilization effects, such as the width of the acceleration region and the heating and energy exchange in the flow. Including the two latter effects yields a theory encapsulated by the Takabe formula [5], which predicts.

$$\gamma = \alpha\sqrt{ka} - \beta kv_{abl} \quad (22)$$

With $\alpha = 0.9$ and β is called *ablative stabilization coefficient* (obtained by fitting to numerical simulations). Takabe set up a true steady-state equilibrium situation with material flow through an absorption region, and numerically found the eigen functions of the flow. This resulted in a best fit to the growth rates. The most widely used growth rate is

$$\gamma = \sqrt{\frac{ka}{1+kL}} - \beta kv_{abl} \quad (23)$$

This is still only an analytical fit to numerical results includes both the ablation velocity and the continuous density gradient effects, where $\beta = 1$ to 3 [5]. The case $\beta = 1$ corresponds to an indirect-drive scenario whereas $\beta = 3$ to the direct-drive case. The term $\beta k v_{abl}$ describes the stabilizing effect of ablation.

2.4. *Rayleigh-Taylor instability in the presence of magnetic field*

In this section, we will study the effects of magnetic field directed parallel to the accelerated interface between two fluids, where the heavier fluid is above the lighter fluid, in RT instability [3]. In high power laser plasma interaction very strong magnetic field is produced. Linearization procedure as done in previous sections is used in this analysis in the presence a magnetic field (Gaussian units) as follows,

$$\vec{B} = \vec{B}_0 + \vec{B}_1 \text{ Where } \vec{B}_0 \text{ is constant and } \frac{|B_1|}{B_0} = 1.$$

On neglecting the electric field \vec{E} relative to the \vec{B} field, the momentum equation of the conducting fluid can be written as

$$\rho \frac{\partial \vec{v}}{\partial t} = -\vec{\nabla} P + \frac{1}{c} (\vec{J} \times \vec{B}) \tag{24}$$

Where ' \vec{v} ' is the fluid velocity, ' ρ ' and ' P ' are density and pressure respectively, ' \vec{J} ' is the electric current and ' c ' is the speed of light. Using the Maxwell equations we have

$$\vec{J} = \frac{c}{4\pi} (\vec{\nabla} \times \vec{B}) \tag{25}$$

The displacement current has been ignored and linearized momentum equation is written as

$$\rho_0 \frac{\partial \vec{v}}{\partial t} = -\nabla P - \frac{\vec{B}_0}{4\pi} \times (\vec{\nabla} \times \vec{B}_1) - g \rho_1 \hat{z} \tag{26}$$

Maxwell equation for zero resistivity is given by

$$\frac{\partial \vec{B}}{\partial t} = -c \vec{\nabla} \times \vec{E} = \vec{\nabla} \times (\vec{v} \times \vec{B}_0) \tag{27}$$

Non existence of magnetic monopole leads towards the expression

$$\vec{\nabla} \cdot \vec{B}_1 = 0 \tag{28}$$

After solving Eqs. (9), (10), (26) and (27) by assuming x, y, t dependence of the variables as in previous case with some algebraic manipulations, we get the following differential equations for the two cases:

Case: 1 When magnetic field is perpendicular to interface of two fluids i.e. $\vec{B}_0 = B_0 \hat{z}$:

$$\left[\frac{d}{dz} \left(\rho_0 \frac{d}{dz} \right) + \frac{B_0}{4\pi\omega^2} \left(\frac{d^2}{dz^2} - k^2 \right) \frac{d^2}{dz^2} \right] u_z(z) = \left[k^2 \rho_0 + \left(\frac{k^2 g}{\omega^2} \right) \frac{d\rho_0}{dz} \right] u_z(z) \tag{29}$$

Case: 2 When magnetic field is parallel to interface of two fluids i.e. $\vec{B}_0 = B_0 \hat{x}$:

$$\left[\frac{d}{dz} \left(\rho_0 \frac{d}{dz} \right) - \frac{B_0 k_x^2}{4\pi\omega^2} \left(\frac{d^2}{dz^2} - k^2 \right) \right] u_z(z) = \left[k^2 \rho_0 + \left(\frac{k^2 g}{\omega^2} \right) \frac{d\rho_0}{dz} \right] u_z(z) \tag{30}$$

In laser-plasma interaction the horizontal magnetic field might play an important role in stabilizing the RTI. In particular, if the large d.c. magnetic field, created in the corona, penetrates into the ablation surface then the ablation surface instability is significantly modified [3]. There is no perturbation propagating in the z-direction, so the stabilizing effects of magnetic field in the z-direction are not taken and only Eq. (30) is further analyzed. On solving Eq. (30) for two uniform fluids separated at the surface $z = 0$, with a density distribution given as

$$\rho(z) = \rho_{up} \theta(z) + \rho_{down} \theta(-z)$$

At the horizontal boundary $z = 0$, the following continuity conditions must be satisfied i.e.

$$\lim_{\varepsilon \rightarrow 0} \{u_z(+\varepsilon) = u_z(-\varepsilon)\}$$

$$\lim_{\varepsilon \rightarrow 0} \{B_z(+\varepsilon) = B_z(-\varepsilon)\}$$

After integrating Eq. (30) along the interface (Integration of magnetic effect term is given in Appendix and integration of other terms is same as in previous cases) and solving Eq. (30) as in previous cases we get

$$\omega^2 = -kg \left[\frac{(\rho_{up} - \rho_{down})}{(\rho_{up} + \rho_{down})} - \frac{B_0^2 k_x^2}{2\pi(\rho_{up} + \rho_{down})gk} \right] \quad (31)$$

Here in this case *Atwood number* is reduced in the presence of magnetic field, which leads towards the reduction of growth rate of RT instability. The *effective Atwood number* in the presence of magnetic field is defined by

$$A' = \left[\frac{(\rho_{up} - \rho_{down})}{(\rho_{up} + \rho_{down})} - \frac{B_0^2 k_x^2}{2\pi(\rho_{up} + \rho_{down})gk} \right] \quad (32)$$

The growth rate ' γ' ' is given by

$$\gamma' = \sqrt{A'kg} \quad (33)$$

If ϕ is the angle between wave vector k and the initial magnetic field B_0 directed along x -axis, then

$$\cos \phi = \frac{k_x}{k} = \frac{k_x}{\sqrt{k_x^2 + k_y^2}}, \text{ where } k = \frac{2\pi}{\lambda} \text{ has been defined.}$$

For stable modes, $\omega^2 > 0$, then from Eq. (27), we have

$$\frac{(\rho_{up} - \rho_{down})}{(\rho_{up} + \rho_{down})} < \frac{B_0^2 k_x^2}{2\pi(\rho_{up} + \rho_{down})gk}$$

which satisfies

$$\lambda < \frac{B_0^2 \cos^2 \phi}{g\Delta\rho} = \lambda_c, \text{ where } \Delta\rho = (\rho_{up} - \rho_{down}) \quad (34)$$

The above expression shows that wavelengths shorter than a critical value λ_c will be stabilized by magnetic field for RTI case.

3. Numerical Results

In order to obtain numerical results to study RTI, we have used different parameters, $\rho_{up} = 10\text{gm/cm}^3$, $\rho_{down} = 1\text{gm/cm}^3$, $a = g = 10^{16}\text{cm/sec}^2$, $B_0 = 10^7\text{Gauss}$, $L = 1.6 \times 10^{-4}\text{ cm}$, $v_{ab} = 3.2 \times 10^5\text{ cm/s}$ described in laser plasma experiments [7].

Using these parameters, it is found that perturbation wavelengths for RTI in laser plasma interactions are in the order of micro-meter (μm) and time for their growth is found to be in the order of nano-second (ns) as shown in the Figures (4-6).

The growth rate vs. perturbation wavelength has been plotted for unmagnetized case, in the absence and presence of density gradient effects at the interface are shown in Fig. 4. If we compare the value of growth rate in both curves, then growth rate is found to be less in the presence of density gradient case for short wavelengths. This behavior shows that density gradient has stabilizing effects for short wavelength perturbations against the RTI which is desirable in experiments. But at large wavelength perturbations, this behavior is found to be opposite and the density gradient stabilizing phenomenon is not more effective to stabilize the RTI as shown in Fig. 4.

Fig. 5 describes the behavior of growth rate with wavelength in the presence of magnetic field $B_0 = 10^7\text{ Gauss}$ (generated in laser plasmas experiments) at different angles of propagation with horizontal direction i.e, for $\phi = 0^\circ, 30^\circ, 45^\circ$ and 60° . After the comparison of growth rate in the case of magnetic field for $\phi = 60^\circ$ with the case when $B_0=0$ as shown in Fig.4, it is found that growth rates in the presence of magnetic field are found be less at small wavelength and are almost same at large values. It is due to the fact that stabilizing behavior of magnetic field is prominent for small wavelengths and become negligible for the large wavelengths.

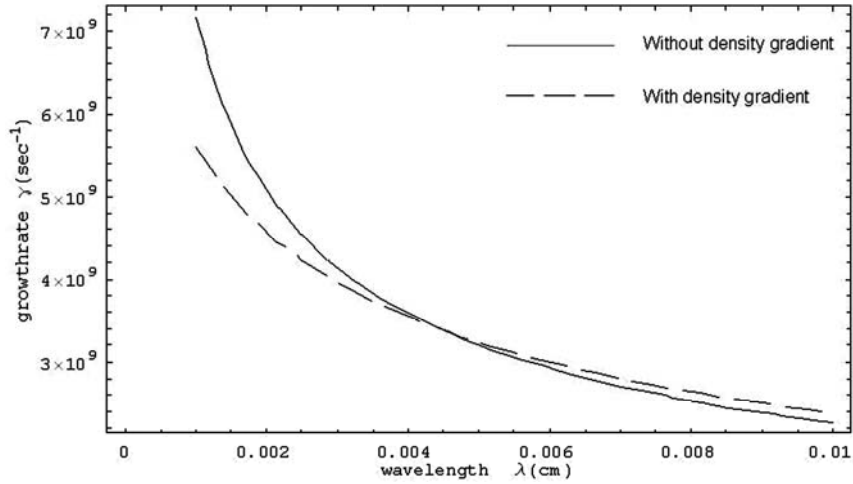


Figure 4. Growth rate Vs wavelength (RTI linear analysis with and without density gradient at the interface).

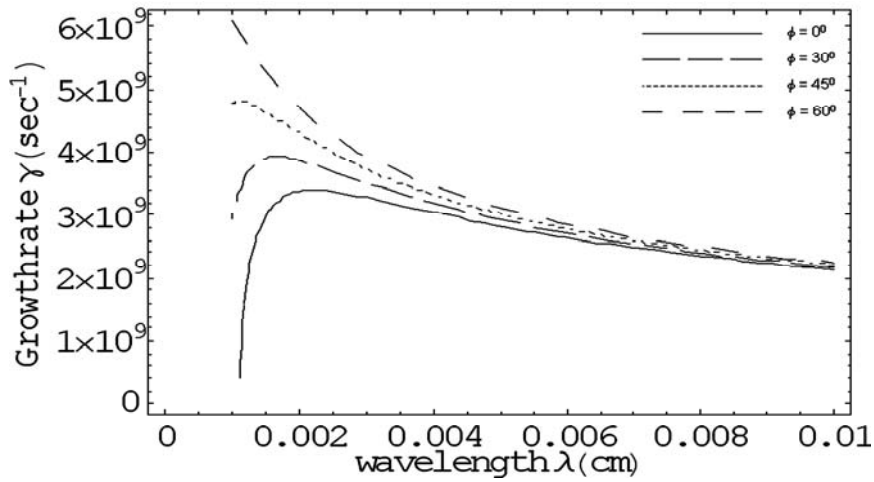


Figure 5. Growth rate Vs Wavelength (RTI analysis with magnetic field for $\phi = 0^\circ, 30^\circ, 45^\circ$ and 60°).

For $\phi = 45^\circ$ it is found that decrease in RTI growth rate at smaller wavelengths is more and similar at large wavelengths in comparison with the case for $\phi = 60^\circ$. In case of $\phi = 45^\circ$, there is a wavelength $\lambda = 10 \mu\text{m}$, for which growth rate is maximum ($\sim 4.8 \times 10^9 \text{s}^{-1}$). The perturbation wavelength has maximum growth rate because the curve has its increasing behavior before that value and after that wavelength it has the decreasing trend.

The RTI growth rates for $\phi = 0^\circ, 30^\circ$ and 45° cases are shown in Fig. 5. The growth rate is the composite behavior of the two terms in Eq.(33) i.e., one is the growth term due to density difference of the fluids and other is the magnetic field effect term as described by effective Atwood number given in

Eq.(32). The behavior of these two terms with wavelength is opposite to each other. At short wave lengths the magnetic field term is more effective in comparison with term containing density difference of the two fluids. For $\phi = 0^\circ, 30^\circ$ and 45° the maximum growth rate is found to be $3.25 \times 10^9 \text{s}^{-1}, 3.9 \times 10^9 \text{s}^{-1}$ and $4.8 \times 10^9 \text{s}^{-1}$ corresponding to the wavelength $\lambda = 20 \mu\text{m}, 16 \mu\text{m}$ and $10 \mu\text{m}$ respectively. From Fig. 5 it is clear that wavelength for which growth rate is maximum, is increased with the decrease in ϕ . Therefore the favorable results are for the case when the angle between the wave vector and magnetic field is minimum because the perturbation in that direction will grow late in comparison with other propagation angle.

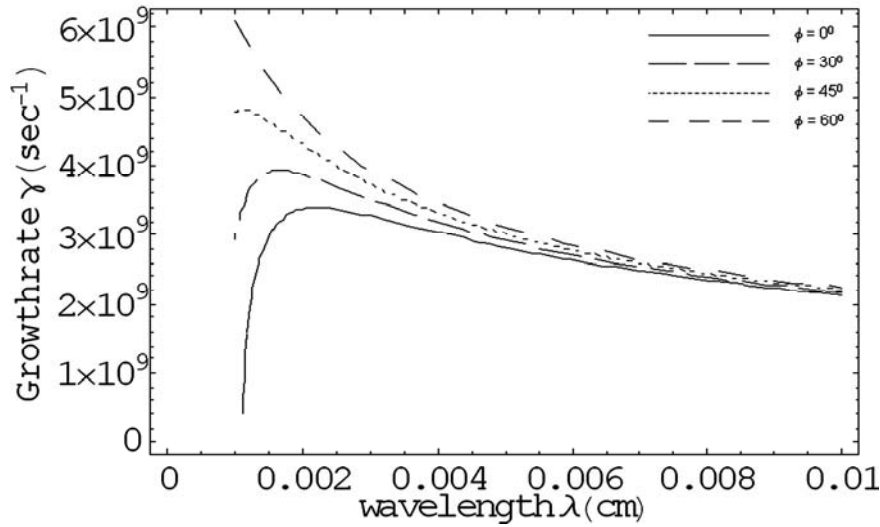


Figure 6. Growth rate Vs wavelength (RTI analysis including density gradient and ablation term for $\beta = 1, 2$ and 3).

The numerical results are also plotted for RTI in the presence of several phenomena during ablation, such as the width of the acceleration region, heating and energy exchange in the flow as given in Eq.(23). Curves for $\beta = 1, 2$ and 3 in Fig. 6 show that the maximum value of growth rate is $3.66 \times 10^9 \text{ s}^{-1}$, $2.65 \times 10^9 \text{ s}^{-1}$ and $2.20 \times 10^9 \text{ s}^{-1}$ at $\lambda = 14 \mu\text{m}$, $26 \mu\text{m}$ and $43 \mu\text{m}$ respectively. The growth rate is composite behavior of the two terms, one is the density gradient term and other is the ablation term as described in Eq. (23). It is found by comparison of growth rates for $\beta = 1, 2$, and 3 as shown in Fig. 6 that with increase in the value of β , the maximum value of growth rate is decreased. For $\beta = 3$ (direct drive case) the maximum value of growth rate is minimum in comparison with other β values. Therefore the case for $\beta = 3$, RTI will take more time to grow and is more favorable in laser plasma experiments.

4. Conclusion

The RTI can cause a disturbance to grow from extremely small amplitude to a level that can disrupt the flow completely and can break the shell in laser produced plasmas. It is found that shorter wavelength modes grow rapidly to reach saturation before the longer wavelength modes because $\gamma \propto \frac{1}{\lambda}$. After the shorter wavelength modes stop growing, they transfer their acquired energy to the longer wavelength disturbances, and

the small disturbances are converted into larger structures [3].

Our results show that density gradient at the interface has a stabilizing effect against RT growth that can reduce the Atwood number and can be explained via an effective Atwood number

$$A = \frac{1}{[1 + kL]} \quad [10].$$

From results it has been clear that in laser-plasma interaction the horizontal magnetic field plays an important role in stabilizing the RT instabilities. It is found that as the angle ' ϕ ' between ' k ' propagation vector and the initial magnetic field (along x-axis) increases, the growth rate stabilizing effect decreases and this effect vanishes when $\phi = 90^\circ$ [3].

Our numerical results show that when we consider ablation of the material surrounding the pellet then growth rate of perturbation is reduced. The physically explanation is that when ablation of the material occurs then there is an additional flow of material across the ablation surface from the high-density region into the low-density plasma which reduces the RTI [9]. Physically ' β ' describes the stabilization effects due to several phenomena occur during ablation, such as the width of the acceleration region, heating and energy exchange in the flow [5]. It is found from

results that the growth rates of the instabilities are also affected by the variations in the value of ' β '. The results are in good agreements with the laser produced plasma experiments [3,5,10].

Appendix

Different Identities Used During Calculations

$$1) \int_{-\varepsilon}^{+\varepsilon} \frac{d}{dz} \rho_0 \left(\frac{du_z}{dz} \right) dz = \rho_0 \frac{du_z}{dz} \Big|_{-\varepsilon}^{+\varepsilon}, \text{ where}$$

$$u_z(z) = \begin{cases} w \exp(+kz) & \text{for } z < 0 \\ w \exp(-kz) & \text{for } z > 0 \end{cases}$$

$$= \rho_0 \frac{du_z}{dz} \Big|_{+\varepsilon} - \rho_0 \frac{du_z}{dz} \Big|_{-\varepsilon}$$

$$= \rho_{up} \frac{d(we^{-kz})}{dz} - \rho_{down} \frac{d(we^{+kz})}{dz}$$

$$= -kw(\rho_{up} + \rho_{down})u_z, \text{ } w \text{ is some constant}$$

$$2) g \frac{k^2}{\omega^2} \int_{-\varepsilon}^{+\varepsilon} (u_z \frac{d\rho_0}{dz}) dz = g \frac{k^2}{\omega^2} [u_z \rho_0]_{-\varepsilon}^{+\varepsilon}$$

$$= g \frac{k^2}{\omega^2} (u_z \rho_0 \Big|_{+\varepsilon} - u_z \rho_0 \Big|_{-\varepsilon})$$

$$= gw \frac{k^2}{\omega^2} (\rho_{up} - \rho_{down}) u_z$$

$$3) \frac{B_0^2 k_x^2}{4\pi\gamma^2} \int_{-\varepsilon}^{+\varepsilon} \frac{d^2(u_z)}{dz^2} dz = \frac{B_0^2 k_x^2}{4\pi\gamma^2} (-\omega k - \omega k) u_z$$

$$= \frac{B_0^2 k_x^2}{4\pi\gamma^2} (-\omega k - \omega k) u_z$$

$$= -\frac{B_0^2 k_x^2 \omega k u_z}{2\pi\gamma^2}$$

$$4) \int_{-\varepsilon}^{+\varepsilon} \frac{k^2 \rho_0 u_z}{\omega} \frac{\partial v_{0z}}{\partial z} dz = \frac{k^2}{\omega} \int_{-\varepsilon}^{+\varepsilon} u_z \rho_0 \frac{\partial v_{0z}}{\partial z} dz$$

$$= \frac{k^2 w}{\omega} \left[\frac{(\rho_{P1} + \rho_{foil}) v_{P1} u_z}{2} \right]$$

Here we have used the symmetry $\delta(z) = \delta(-z)$

$$\text{and } \int_{-\varepsilon}^{+\varepsilon} \theta(z) \delta(z) dz = \frac{1}{2} \text{ (Integration by parts)}$$

$$\text{with } \frac{d\theta(z)}{dz} = \delta(z).$$

References

- [1] N.A. Krall and A. W. Trivelpiece, Principles of Plasma Physics, McGraw-Hill, New York (1973).
- [2] S. Atzeni and J. Meyer-Ter-Vehn, The Physics of Inertial Fusion, Oxford University Press, New York (2003).
- [3] S. Eliezer, The Interaction of High - Power Lasers with Plasmas, Institute of Physics Publishing, London, UK (2002).
- [4] S. Atzeni, Atoms, Solids and Plasma in Super Intense Laser Fields, Kluwer Press, New York, (2001).
- [5] S. Pfalzner, An Introduction to Inertial Confinement Fusion, Taylor & Francis, New York, (2006).
- [6] K. S. Budil, B. A. Remington, T. A. Peyser, K. O. Mikaelian, P. L. Miller, N. C. Woolsey, W. M. Wood-Vasey and A. M. Rubenchik, Phys. Rev. Lett. **76** (1996) 4536.
- [7] J. D. Kilkenny, S. G. Glendinning and S. W. Haan, Physics of Plasmas **1** (1994) 1379.
- [8] G. K. Parks, Physics of Space Plasma An Introduction, 2nd Edition, Westview Press, USA (2004).
- [9] V. N. Goncharov, P. McKenty and S. Skupsky, Physics of Plasmas **7** (2000) 5118.
- [10] R. Betti, V. N. Goncharov, R. L. McCrory and C. P. Verdon, Physics of Plasmas **5** (1998) 1446.
- [11] T. Watari, M. Nakai, H. Azechi, T. Sakaiya and K. Mima, Physics of Plasmas **15** (2008) 092109.